COMBINATORIAL DISCOVERY OF PHOTOCATALYSTS FOR HYDROGEN PRODUCTION

Theodore Mill, Albert Hirschon, Michael Coggiola and Brent MacQueen
SRI International
333 Ravenswood Avenue, Menlo Park, CA 94025

Nobi Kambe and Benjamin Chaloner-Gill
NanoGram Corporation
46774 Lakeview Boulevard, Freemont, CA 94538

ABSTRACT

This report summarizes the activities of a project initiated in September 2001 for the development of tools for the combinatorial analysis of materials with respect to the photocatalytic water splitting to generate hydrogen. As this project is just beginning the majority of the initial effort has been in developing prototype analysis modules and assembling the necessary optical, electrochemistry, sampling and analysis equipment. The prototypes for the photoelectrochemical analysis of materials, has been divided into a module for the analysis of nano-particulate suspensions and for monoliths. In the case of the powder suspensions each photolysis cell contains a micropressure transducer and a sampling port for collection of headspace gas for GC analysis. The signal from the micropressure transducer will initiate the autosampling of the headspace gas by an in house modified Gilsen sample handler. In the case of the monolith samples a design that incorporates the ability to make an ohmic contact and hence monitor electrochemical response of the sample has been developed. These tools will then be used to screen materials generated by our partner, NanoGram Corporation, using their proprietary nanoparticulate synthesis.

INTRODUCTION

The use of water-derived hydrogen as a fuel has been a long-term goal of DOE. The environmental benefit of replacing hydrocarbons with hydrogen as a fuel would be substantial. The largest single source of air pollution in the United States is in the generation and consumption of energy. Two-thirds of all carbon-based emissions result from the burning of fossil fuels for transportation and generation of electricity. To reduce these carbon-based emissions and other harmful pollutants such as NO_x and SO_x a transition must be made from fossil fuel-based technologies to renewable energy. Certainly, this transition will have to occur to meet the DOE goals of reducing carbon emissions by 1.9 million tons by 2010 and 13.5 million tons by 2020. Other goals are to reduce NO_x by 52,000 tons/year, CO by 390,000 tons/year and CO_2 by 45.6 million tons/year by the year 2020. [1]

An abundant renewable energy resource is hydrogen, and the ability to harvest it will be of critical importance in meeting the goals of DOE. Furthermore, the technologies required to implement hydrogen as both an electricity and transportation fuel already exist. As such there are no technical showstoppers to prevent the near-term implementation of hydrogen as a fuel.

However, considerable milestones have yet to be achieved before DOE can realize the goal of using hydrogen as a fuel can be realized. These milestones include the development of economical and environmentally benign hydrogen production methods and reliable storage systems. Despite intense research efforts, few semiconductors and electrocatalysts have been identified as capable of producing hydrogen from water under solar radiation, and those that have been identified have been inefficient or difficult to use on a commercial scale. Breakthrough methods are needed to synthesize new materials rapidly with appropriate band-gaps and screen them for efficient hydrogen production.

The goal of this effort is the economical and environmentally sound production of hydrogen via the photolytic splitting of water. SRI is developing a combinatorial approach to identify semiconductor substrates, surface modification(s), and experimental conditions that lead to the efficient splitting of water to produce hydrogen. Our specific objective in Year 1 of this effort is to develop and validate a combinatorial workstation that can be used to screen an array of materials in terms of electrochemical properties and photocatalysis. Using the workstation and the materials to be supplied by NanoGram, we will screen a number of materials for catalytic characteristics.

The fundamental processes involved in the photolytic splitting of water are the generation of an electron hole pair by the illumination of a semiconductor with photons of energy greater than the semiconductor band gap energy and the transport and consumption of the electron hole pair at the semiconductor electrolyte interface. [2] The key parameters to be considered in the selection of a semiconductor are the band gap energy, which must be greater than the 1.23 V needed to drive electrolysis of water. The efficiency of the photolytic system is a combination of the efficiencies of the two components; that is, charge separation within the semiconductor and the process by which the charge is consumed.[3-6] The efficiency of the generation of the electron hole pair is related to the recombination process that occurs within the space charge region of the semiconductor and competes with the charge transport process that leads to charge ejection. Improvements in the generation of the electron hole pair are thus related to the composition of the semiconductor materials in the space charge region. The efficiency of the charge consumption at the semiconductor electrolyte interface is related to the thermodynamic barrier and reorganizational energies associated with the charge transfer process. These processes manifest themselves in the form of an overpotential required to drive the corresponding redox process. Thus, the process to be optimized for improved efficiency is a reduction of the overpotential required to drive the redox process of choice. This is typically facilitated by the use of a catalyst. Furthermore, it is important that charges, either electrons or holes, not be allowed to build up on the surface of the electrode as this will allow for corrosion of the semiconductor and a subsequent loss in efficiency.

The combinatorial approach that SRI and NanoGram are developing will allow for the investigation of the optimization of both efficiency factors described above. That is, we will be able to conduct a systematic analysis of the compositional effect of the semiconductor materials as related to charge generation. Using NanoGram's proprietary particle synthesis technology, we will prepare an array of materials with significant variations in atomic composition, size and phase. Using the combinatorial photoelectrochemical array that SRI will develop during the course of this effort, we will be able to screen these materials in a rapid fashion, allowing for the identification of potential new semiconductor materials. At the same time, SRI will be able to screen a number of electrocatalysts that could lead to a reduction in the overpotential for hydrogen generation. The overall goal of the effort is thus the identification of new semiconductor substrates as well as the identification of efficient catalysts. The combination of

the two efforts should lead to the development of an optimized photolytic system for the economic and environmentally friendly production of hydrogen.

EQUIPMENT

Light Source

Assembly of 1 kW Solar Simulator

A 1 kW solar simulator was assembled by coupling an Oriel 1 kW xenon lamp with its associated housing and power supply to a full reflecting front surface mirror through a condenser, water filter and electronic shutter (all from Oriel). This assembly was positioned on the floor below a bench top with a circular opening through which the light projects onto the bottom of a reaction cell. The light beam is reflected upwards from the mirror through a beam turner and through first a 7.6 cm lens and then through a secondary 20 cm (8 in) collimating lens to impinge on a flat borosilicate plate on the bench top opening. At this point, all light below 290 nm and most light above 900 nm has been removed through the combination of the water filter and borosilicate plate.

Calibration of Solar Simulator

To determine both the intensity and intensity distribution of simulated sunlight at the top of the borosilicate plate, two kinds of light intensity measurements were made using both irradiance measurements with a International Light radiometer (Model IL1400A with a solar active probe (SEL033) and photon intensity measurements with a chemical actinometer added to each of the four cells.

The xenon lamp was turned on and warmed up for 30-60 minutes before any measurements were made. A poly(methylmethacrylate) (PMMA) cell block (see Figure 4 for picture of cell block) was centered on top of the Pyrex sheet and fiduciary marks were made to the block and sheet to ensure reproducible positioning in the future. Cells were numbered 1-2 top and 3-4 bottom. An arrow on the block points to the top.

Radiometry on the cells was performed with a 1 mm pinhole aperture in the solar probe. The radiometer was zeroed and the probe then centered over each of the four cells while power readings were made (in mW/cm^2). The probe was scanned a few mm to the right, left, top and bottom of each cell to get a range of irradiance readings in each cell. The values varied a little with an average of 51 ($\pm$ 1-2) mW/cm^2 over the face of the cells. These values are shown in Table 1 below.

Table 1: Calibration Data for Four-Cell Block with 1 kW Xenon Lamp

Cell #	1	2	3	4
Power mW/cm^2 1 st meas.	48 $\pm$ 1	52 $\pm$ 0.5	53 $\pm$ 1	51.5 $\pm$ 1.5
Power mW/cm^2 2 nd meas	46 $\pm$ 1	51 $\pm$ 1	53 $\pm$ 1	51 $\pm$ 0.5
.Rate constants for photolysis with AZB in Ms^{-1}	3.20×10^{-4}	3.45×10^{-4}	3.74×10^{-4}	3.63×10^{-4}

Actinometry was performed on the cell block using four 3-mL aliquots of 100 µM azoxybenzene [7] in EtOH added to the cells for 3, 7, 11 and 16 minute exposures to the xenon lamp. This volume of AZB ensures that all light around 325 nm is absorbed by the AZB solution. After each time exposure, the solutions were removed from the cells and new solutions were added for a

total of 16 AZB samples that were analyzed by UV at 458 nm for the AZB photoproduct. The results were plotted using the relation

$$\ln(1-P/A_0) = I_0\Phi t/ A_0 \qquad (1)$$

where A_0 is the original concentration of AZB, P is the concentration of the product 2-hydroxyazobenzene (measured by UV), I_0 is the absorbed radiation intensity in photons/s and Φ is the quantum yield (0.04). A plot of $\ln(1-P/A_0)$ versus t for each cell gave the linear relations shown in Figure 1 with slopes of $I_0\Phi/ A_0 = k_p$. The relative changes in rate constants k_p for photolysis from cell to cell compared well with the changes in radiometer values in mW/cm^2 from cell to cell. The values are shown in Table 1.

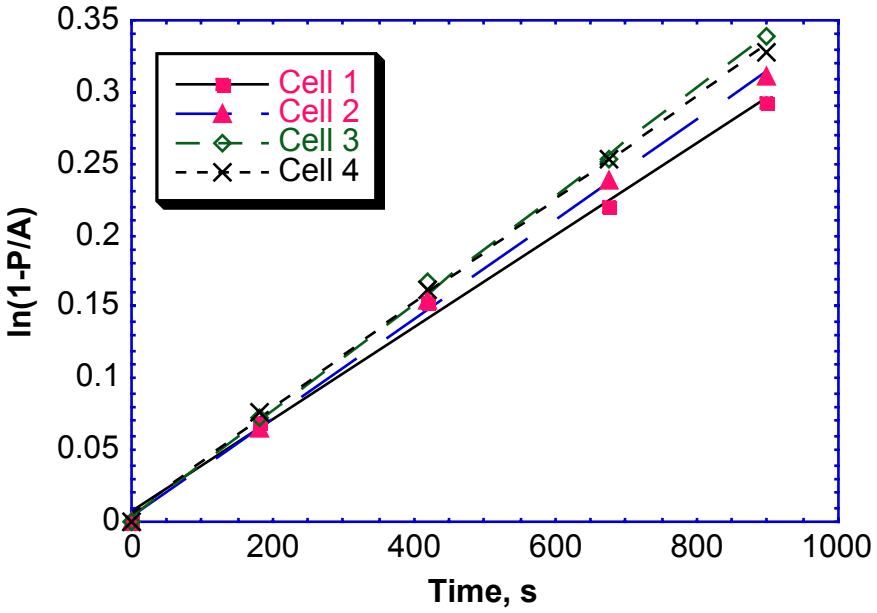

Figure 1. Plot of Equation 1 for AZB loss with the solar simulator

For comparison, radiometer values for sunlight gave 71-76 mW/cm^2 for March 8 sunlight at 130 p.m. or about 70% higher than for the solar simulator. In another comparison, Loss of AZB, irradiated in sunlight on 21 Feb 2002 near noon under clear skies has a rate constant of 2.06 x 10^{-3} Ms^{-1} (see Fig 2 for a plot of the data), or about 6 times larger than loss rates for AZB in the solar simulator. The much lower AZB loss value for the simulator might be associated with several factors, including the way the sunlight experiment was conducted: quartz tubes with AZB solutions collected both direct sunlight and skylight, whereas the cells on the simulator see the collimated beam only. Typically, skylight comprises only about 50% of the total solar irradiance.

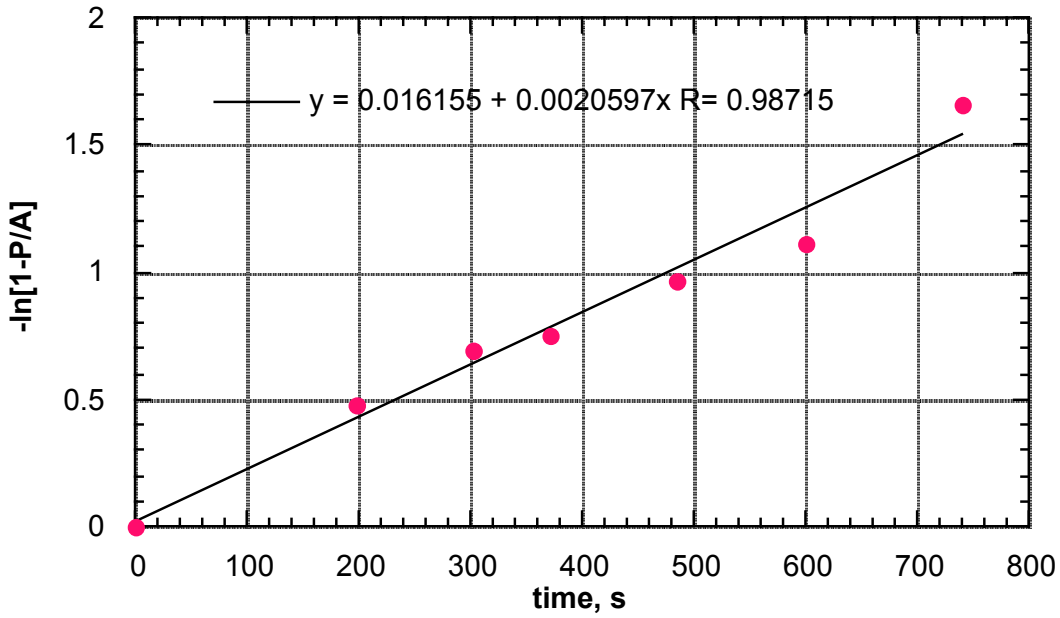

Figure 2. Plot of Equation 1 for AZB loss in sunlight

The calibration experiments show that the simulator is producing a fairly uniform light field for the 10 x 10 cm cell block with about 70% of the irradiance measured by the radiometer when it was aimed directly at an early March sun under clear skies near solar noon. AZB actinometry measures the photon intensity around 325 nm in the near UV where AZB absorbs light. The larger differences found here between sunlight and simulated sunlight intensities using AZB (up to a factor of three) may reflect an inherently lower photon flux in the near UV region in the simulator light field compared with the visible region which the radiometer measures. Some actinometry measurements using an actinometer absorbing in the visible region may be useful for clarifying the reasons for the differences seen here.

ANALYSIS MODULES

Powder Module

The analysis modules have been designed to look at both particulate suspensions and monolithic substrates. In the case of suspension the initial 4 cell module is composed of an acrylic base with Quartz windows mounted in the bottom of 2 cm diameter wells. O-ring grooves are machined into the top of the base to allow the top plate to seal to the base thus isolating each cell. In our initial design, Figure 3, we had separate inlet and outlet purge lines, a pressure transducer attachment and a separate septum inlet for head space sampling. All of this hardware on the top of the cell proved to be too cumbersome as well as a concern that the cells may not remain hermetically sealed with four separate ports being placed through the top plate.

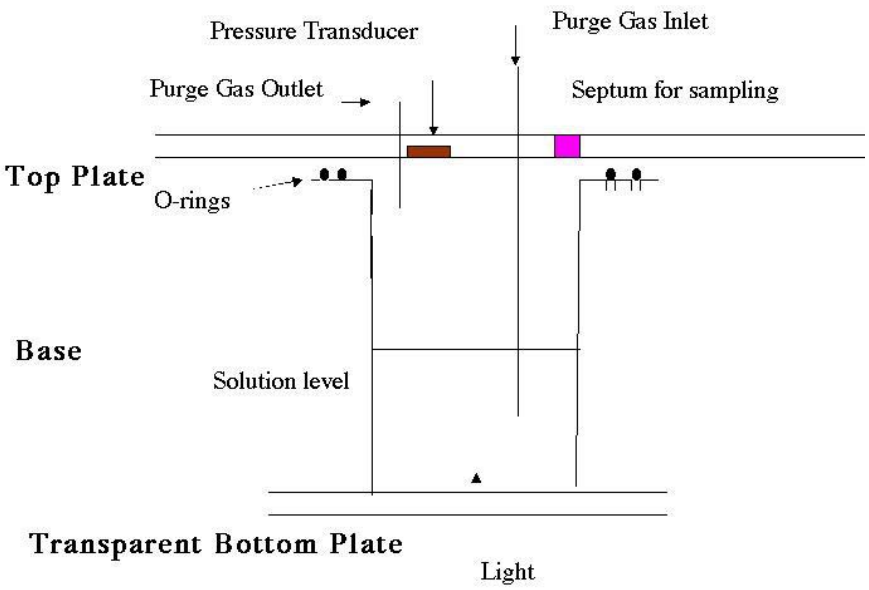

Figure 3. Drawing of initial concept for powder analysis module

As a result of the concerns expressed above we changed the top plate design to a single threaded inlet to which a swagelok fitting was set that contained a septum on the top and a sidearm to which the pressure transducer was attached, Figure 4. The module is loaded in a nitrogen box, which alleviates the need for an initial purge to remove oxygen, and subsequent purges required for long term experiments can be facilitated via the Gilsen sampler.

We have designed an expanded powder analysis module to a 25-cell unit that fits within our 8 inch diameter solar simulator. Refinement of this design is in progress.

Monolith Module

We have also designed an analysis module for the investigation of monolithic substrates. In this case ohmic contact can be made to the substrate and hence information can be obtained using standard electrochemical approaches. The working electrode in the module, see partial drawing in Figure 5. Is designed such that it will screw into the top of the base for the monolith analysis module. The current design has a removable substrate assembly such that substrates can be easily interchanged once ohmic contact to the metallic plate within the assembly is established.

The base of the monolith analysis module is similar in dimensions to the 4-cell powder unit previously discussed with the exception that each cell now contains a ring of glassy carbon that serves as a counter electrode and a silver wire that is either a pseudo reference or converted to Ag+/AgCl reference electrode. Thus each individual cell has its own working, counter and reference cell. The design is currently being refined and we expect to report on the results of an initial 4-cell unit and its expansion in our next semiannual report. At that time we will also report on the electrochemical set up we have assembled to conduct those experiments. This equipment includes an Arbin multi-cell analyzer, several PAR potentiostats and a four channel Solartron frequency response analyzer.

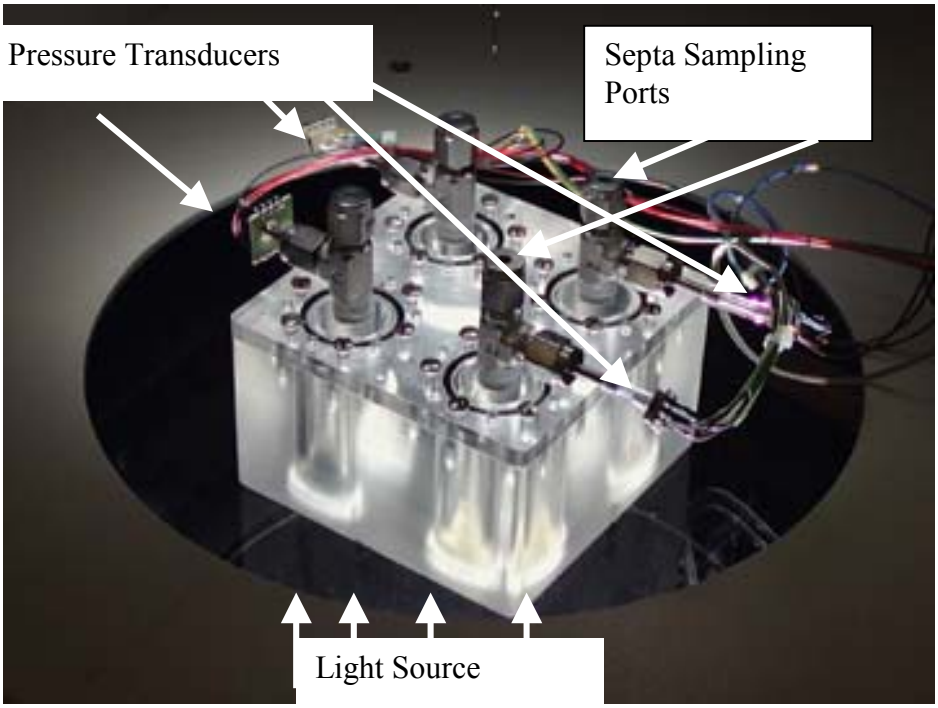

Figure 4. 4-cell module for analysis of powder photocatalytic activity.

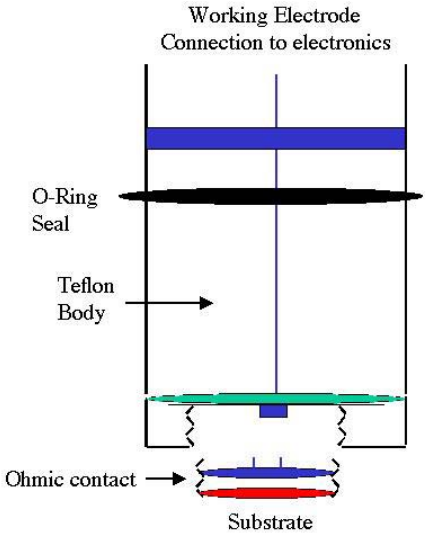

Figure 5. Working electrode assembly for monolith analysis module

Pressure Measurements

Pressure measurement on the prototype cells is performed using individual solid-state pressure sensors. Initially, three different commercial sensors are being evaluated, as summarized in Table 2.

Table 2. Commercial pressure transducers investigated

Manufacturer	Model	Full Scale	Output
Silicon Microstructures (Fremont, CA)	SM5350-008	0.8 psig	50 mVdc
Silicon Microstructures (Fremont, CA)	SM5310-005	5 psig	100 mVdc
Lucas NovaSenor (Fremont, CA)	NPC-410-005	5 psig	125 mVdc

Each sensor is a Wheatstone bridge configuration that is powered by a constant voltage source (5 Vdc) and produces an output voltage proportional to the inlet pressure. Because of the bridge configuration, the output voltage must be measured using a system with a differential (floating) input. A preliminary voltage measuring workstation has been assembled using a conventional Intel-based PC equipped with an 8-channel (differential), 12-bit, analog-to-digital (ADC) converter.

A simple, Windows-based, application has been developed to facilitate reading and recording the cell pressures. The application sequentially reads the sensor outputs via the ADC at a constant rate of 1 Hz. The data is displayed in absolute pressure units on the terminal, however, no data is recorded until the user initiates a run. Before starting a run, the user can select an interval between 1 and 10 seconds in which data will be recorded. The user also has the option of choosing the format in which the data will be saved; either as a tab-delimited text file or inserted directly into an Excel spreadsheet. Once the run begins, the time in seconds and each cell's pressure reading are recorded. Data accumulation continues until manually halted by the user.

Future pressure measurements will be made using the same basic configuration, although only a single sensor type will be employed. A new 32 channel (differential), 14-bit ADC has been purchased to expand the number of cells that can be monitored. The software is modular and can easily be reconfigured for the larger cell count.

A sample data set collected during initial testing of the powder analysis module is shown in Figure 6. The data shown are for commercial samples of niobate (Alfa Aesar) with a nickel catalyst, P25 titania with a platinum catalyst and tris- (2,2'-bipyriidine)ruthenium(II) as a sensitizer and a blank cell with titania powder without a catalyst.

We have also received some samples of some extremely small pressure transducers from Silicon Microstructures. The size of theses devices (3 x 3 mm) will allow for reduction in the size of the cell volume which will result in a higher cell density per module.

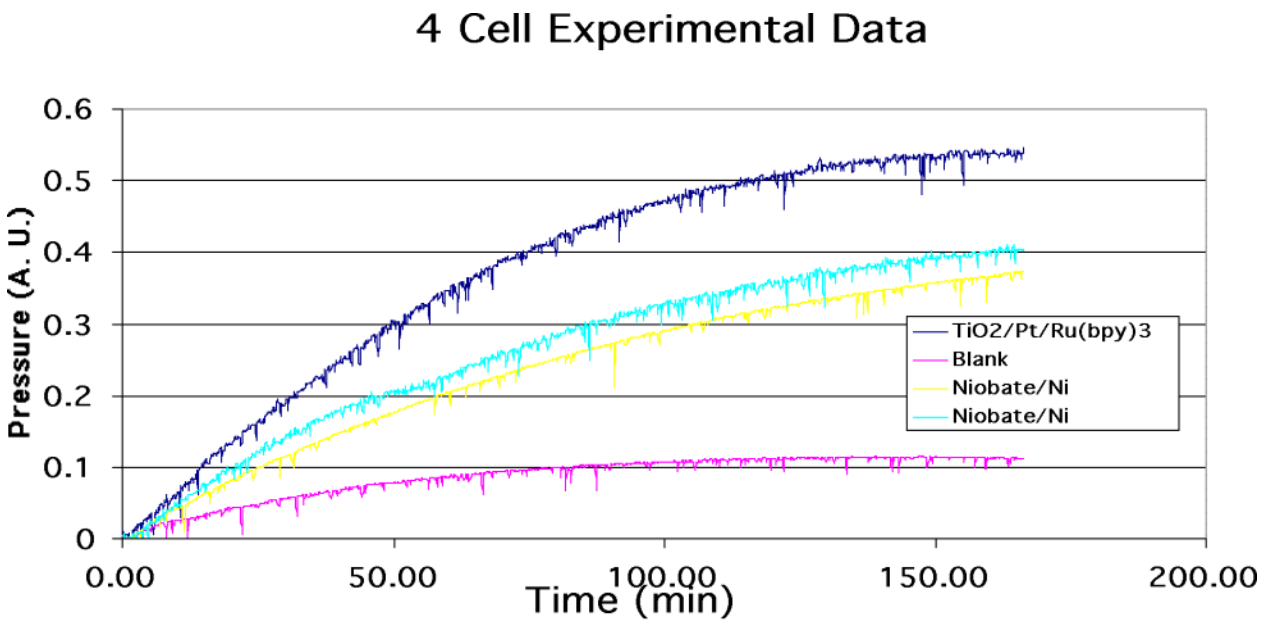

Figure 6. Pressure transducer data from 4-cell powder analysis module

Headspace Sampling and Analysis

Several designs were considered for sampling of the head gases during the photolysis experiment. It was determined that commercial headspace analyzers are not compatible with the photolysis cell design unless modification of the analyzers was done. Specifically, problems with the commercially available analyzers involved syringe control and depth. The commercial companies SRI contacted were not willing to modify their equipment at a cost that would be compatible with available project funds. An alternative design was made using a commercial pipetor as a means of controlling the sampling syringe. A Gilson sampler, previously purchased by SRI, was modified for the sampling system. Several types of detectors for hydrogen and oxygen were considered specifically mass spectroscopy, MS, and gas chromatography, GC.

For the purposes of the first year of the project we decided to use an existing GC for these analyses. As progress continues in the developments in MEMS based gas sensors by other groups within the Hydrogen Program, and without, we anticipate the incorporation of these devices directly with each photolysis cell, with a micro-pressure transducer, as described earlier. The incorporation of these MEMs devices into the cell will negate the need for direct interrogation by a probe as well as to allow for smaller cell volumes and hence a higher cell density with an analysis module.

PARTICLE SYNTHESIS

NanoGram utilizes lasers in its production of inorganic, crystalline nanomaterials. The NanoGram™ process for producing nanoparticles is based on Laser-driven chemical reaction that takes place within a well-controlled reaction zone. A CO_2 Laser beam provides a heat source for rapid heating (at a rate on the order of 10^5 K/sec) within a tiny and controlled reaction zone, resulting in high-temperature pyrolysis and chemical reaction between the precursors. Immediately after the Laser reaction zone, nanoscale particles are formed due to a rapid cooling

(at a rate on the order of 10^5 K/sec) without any contact with a cooling agent. This process occurs essentially at nonequilibrium. In contrast to conventional processes, which either grinds large particles into small particles or use poorly controlled reaction vessels, NanoGram virtually builds nano-scale particles from the atomic level. This patented method is the best process for manufacturing nanomaterials as measured by quality, purity, composition control, particle-size control and cost effectiveness. The company can produce a wide range of crystalline nanomaterials including oxides, carbides, sulfides, nitrides, phosphides and silicates, as well as complex materials made of three or four (or more) elements, called ternary and quaternary materials. The process can produce the widest range of end-product compounds and utilize a full complement of lower cost, commodity chemicals as feed stocks.

NanoGram has developed an efficient chemical reaction process inside a chamber by optimizing an equipment design and a flow control of precursors and particle collection [8]. As a result, throughputs up to 1 kg/hour of production for several test compounds have been demonstrated. Process scale-up work is ongoing with substantial results achieved already. Current process design modifications are expected to deliver another throughput increase in the range of 10-20X (to approximately 4 kg/hr).

NanoGram's reactor setup is shown in Figures 7 and 8. A TEM and some XRD data of NanoGram produce powders are shown in Figures 9 and 10. As this data shows NanoGram can effectively control the phase of TiO_2 that is produced using their proprietary particle synthesis technology. We have just recently received our first lot of samples from Gram hese materials now. After establishing some baseline activity for these materials will start the modification and analysis of the nanoparticulates in earnest over the next half of this fiscal year.

SUMMARY

In summary we have made a great deal of progress in assembling the components necessary to conduct high throughput screening of materials for photocatalytic generation of hydrogen from water. This includes building a solar simulator, assembling and modifying the sample collection and sample analysis equipment and the design and construction of analysis cells. There has been a delay in the start of the sample analysis due to a relocation of NanoGram to a larger facility. However, that move is complete, powders are being delivered and we look forward to disseminating our results in the next report.

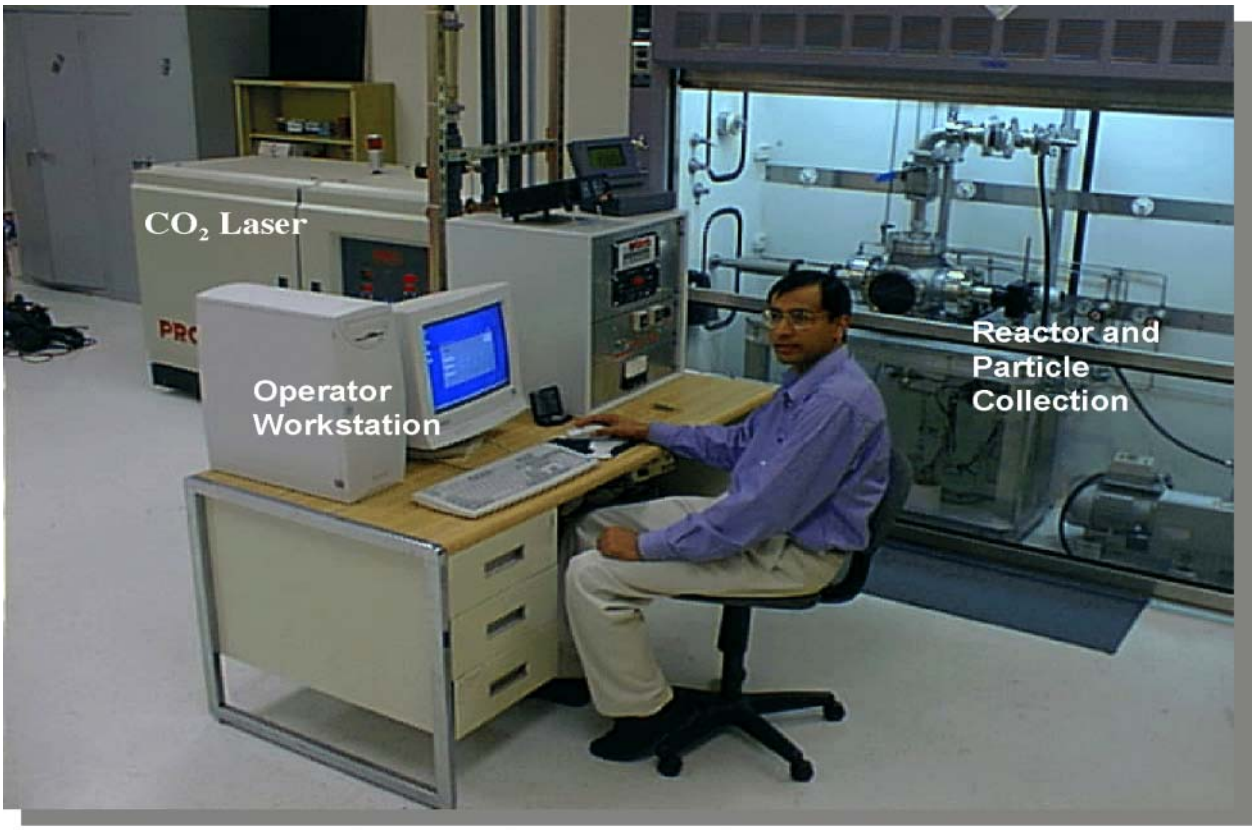

Figure 7: NanoGram particle synthesis apparatus

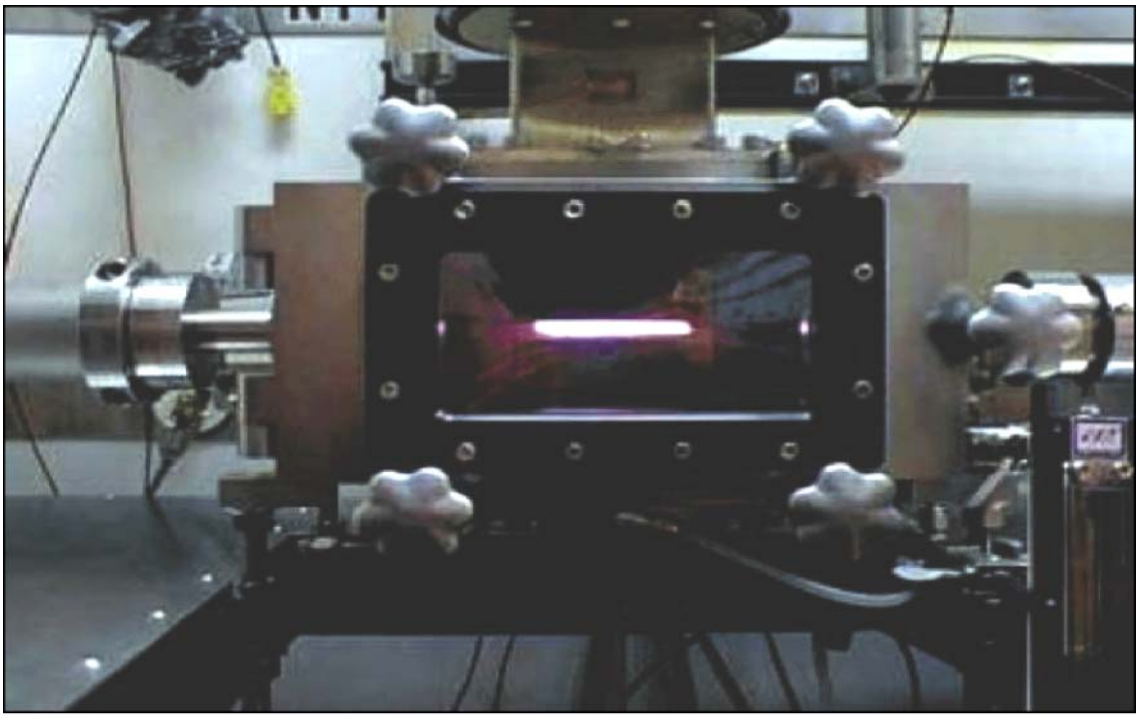

Figure 8: Closeup of reaction zone in NanoGram reactor

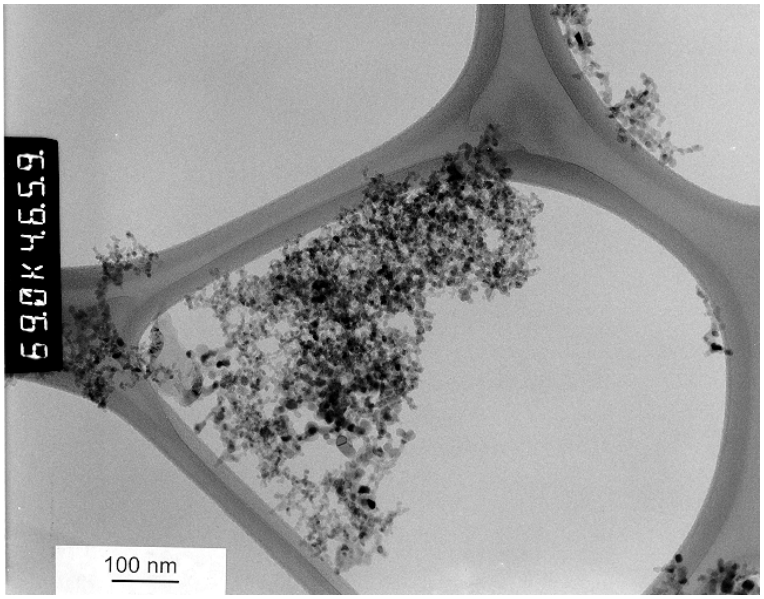

Figure 9. TEM of NanoGram produced TiO2

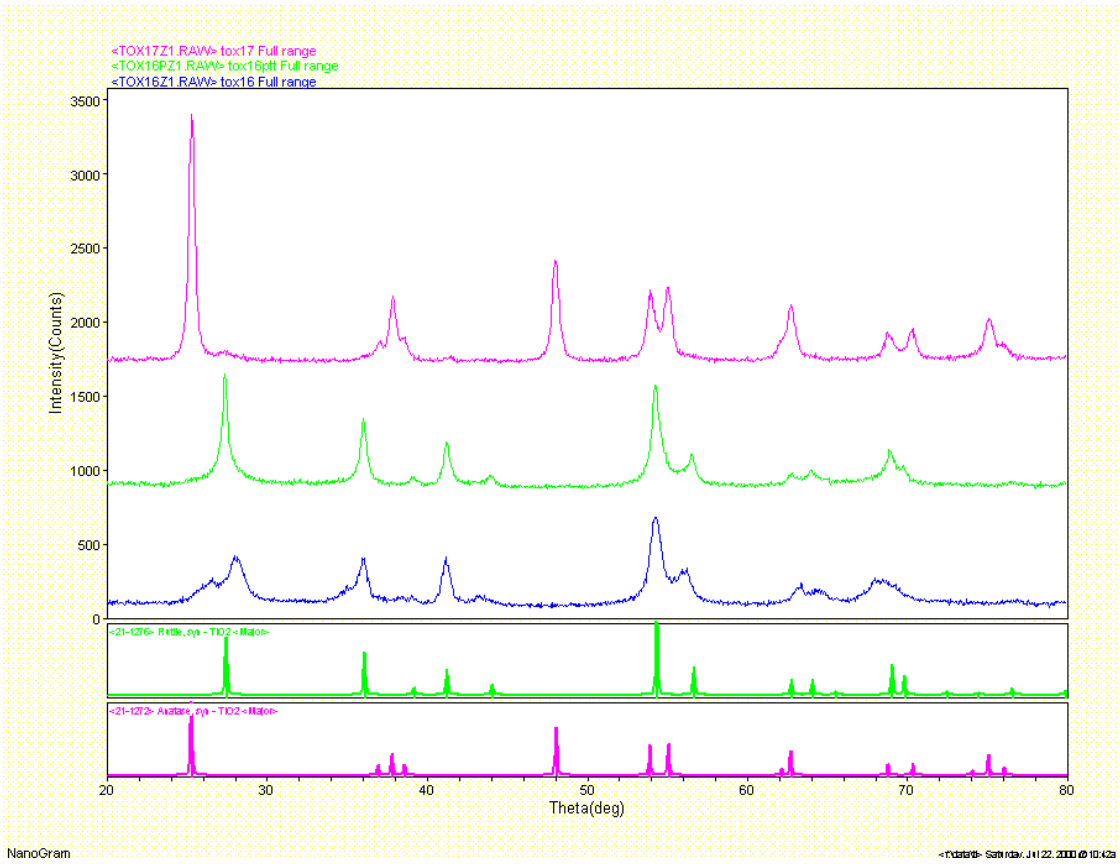

Figure 10. XRD of NanoGram produced titania powders showing rutile, anatase and a mixed phase material

REFERENCES

1. Gronich, S., N. Rossmeissl, and C. Bordeaux, *FY 2001 Annual Operating Plan—Hydrogen Program*, U.S. Department of Energy **2000**.
2. Gerischer, H., "Solar Photoelectrolysis with Semiconductor Electrodes," Topics in Applied Physics Volume 31, Solar Energy Conversion, Solid State Physics Aspects, Ed. By B. O. Seraphin, 115-172.
3. Bolton, J. R., Strickler, S. J. and Connolly, J. S. " Limiting and Realizable Efficiencies of Solar Photoloysis of Water," *Nature*, **1985**, 316, 495-500.
4. Licht, S., B. Wang, and S. Mukerji, "Efficient Solar Water Splitting, Exemplified by RuO_2-Catalyzed AlGaAs/Si Photoelectrolysis," *J. Phys. Chem. B* **2000**, *104*, 8920-8924.
5. Duonghong, D., E. Borgarello, and M. Gratzel, "Dynamics of Light-Induced Water Cleavage in Colloidal Systems," *J. Amer. Chem. Soc.* **1981**, *103*, 4685-4690.
6. Takata, T., A. Tanaka, M. Hara, J. N. Kondo, and K. Domen, "Recent Progress of Photocatalysts for Overall Water Splitting," *Catalysis Today* **1998**, *44*, 17-26.
7. Bunce N J, J LaMarre, SP Vaish. "Photorearrangement of azoxybenzene to 2-hydroxyazobenzene: a convenient chemical actinometer". *Photochem Photobiol* **1984** *39*, 531-533.
8. Bi, X and N. Kambe, US Patent 5,958,348 (1999).